



Brief Paper

Calibration and estimation of redundant signals[☆]Asok Ray^{a,*}, Shashi Phoha^b^aMechanical Engineering Department, The Pennsylvania State University, University Park, PA 16802, USA^bApplied Research Laboratory, The Pennsylvania State University, University Park, PA 16802, USA

Received 3 June 1999; revised 18 October 1999; received in final form 1 February 2000

Abstract

This paper presents formulation and validation of an adaptive filter for real-time calibration of redundant signals consisting of sensor data and/or analytically derived measurements. The measurement noise covariance matrix is adjusted as a function of the a posteriori probabilities of failure of the individual signals. An estimate of the measured variable is obtained as a weighted average of the calibrated signals. The weighting matrix is recursively updated in real time instead of being fixed a priori. The calibration and estimation filter has been tested by injecting faults into the data set collected from an operating power plant. The filter software is presently hosted in a Pentium platform and is portable to other commercial platforms. The filter can be used to enhance the Instrumentation & Control System Software in tactical and transport aircraft, and nuclear and fossil power plants. © 2000 Elsevier Science Ltd. All rights reserved.

Keywords: Adaptive filtering; Real-time control; Redundancy management; Sensor calibration; Signal estimation

1. Introduction

Redundant sensors are often installed to generate spatially averaged time-dependent estimates of critical variables for reliable monitoring and control of complex dynamical processes such as aircraft (Daly, Gai & Harrison, 1979) and power plants (Deckert, Fisher, Laning & Ray, 1983). Sensor redundancy is often augmented with analytical measurements that are obtained from physical characteristics and/or model of the plant dynamics in combination with other available sensor data (Desai, Deckert & Deyst, 1979; Ray, Geiger, Desai & Deyst, 1983; Ray & Desai, 1986). Both sensor and analytical redundancies are referred to as redundant signals in the sequel.

Individual signals in a redundant set may often exhibit deviations from each other after a length of time. These differences could be caused by slowly time-varying sensor parameters (e.g., amplifier gain), plant parameters (e.g.,

structural stiffness, and heat transfer coefficient), transport delays, etc. Consequently, some of the redundant signals could be deleted by a fault detection and isolation (FDI) algorithm if these signals are not periodically calibrated. On the other hand, failure to isolate a degraded signal (for example, due to increased threshold bound in the FDI algorithm) could cause an inaccurate estimate of the measured variable. In this case, the plant performance and stability may be adversely affected if the inaccurate estimate is used as an input to the decision and control system.

This paper presents a calibration and estimation filter for redundancy management of sensor data and analytical measurements. The salient features of the filter are delineated below.

- All signals are simultaneously calibrated on-line to compensate for their relative errors.
- The weights of individual signals for computation of a least-square estimate of the measured variable are adaptively updated as functions of the respective a posteriori probabilities of failure.

In the event of an abrupt disruption of a redundant signal in excess of its allowable bound, the respective signal is isolated by the FDI algorithm, and only the remaining signals are calibrated to provide an unbiased

[☆]This paper was not presented at any IFAC meeting. This paper was recommended for publication in revised form by Associate Editor M. Basseville under the direction of Editor Torsten Söderström.

* Corresponding author. Tel.: +1-814-865-6377; fax: +1-814-863-4848.

E-mail address: axr2@psu.edu (A. Ray).

estimate of the measured variable. For a gradual degradation (e.g., a sensor drift), the faulty signal is not immediately isolated but its influence on signal calibration and estimation is diminished as a function of its deviation from the remaining signals. This is achieved by decreasing the relative weight of the degraded signal as a monotonic function of the magnitude of its residual (i.e., deviation from the estimate) that is a measure of its relative degradation. Thus, if the error bounds of the FDI algorithm are appropriately increased to reduce the probability of false alarms, an undetected fault would have smaller bearing on the accuracy of signal calibration and estimation as a result of the adaptively reduced weight. Therefore, the resulting delay in detecting a gradual degradation could be tolerated because the weighted estimate is practically unaffected. Furthermore, since the weight of a gradually degrading signal is smoothly reduced, the eventual isolation of the fault would not cause any abrupt change in the estimate.

The calibration and estimation filter is validated based on redundant sensor data of throttle steam temperature collected from an operating power plant. Development and validation of the filter algorithm are presented in the main body of the paper along with concluding remarks. The appendix presents the theory of multiple hypotheses based on a posteriori probability of failure of a single signal.

2. Signal calibration and estimation

A redundant set of ℓ sensors and/or analytical measurements of a n -dimensional plant variable are modeled at the k th sample as

$$m_k = (H + \Delta H_k)x_k + b_k + e_k, \quad (1)$$

where m_k is the $(\ell \times 1)$ vector of (uncalibrated) redundant signals, H the $(\ell \times n)$ a priori determined matrix of scale factor having rank n , with $\ell > n \geq 1$, ΔH_k the $(\ell \times n)$ matrix of scale factor errors, x_k the $(n \times 1)$ vector of true (unknown) value of the measured variable, b_k the $(\ell \times 1)$ vector of bias errors, and e_k the $(\ell \times 1)$ vector of measurement noise, such that $E[e_k] = 0$ and $E[e_k e_k^T] = R_k \delta_{kl}$.

Remark 1. The noise covariance matrix R_k of uncalibrated signals plays an important role in the adaptive filter for both signal calibration and estimation. Later it is shown how R_k is recursively tuned based on the history of calibrated signals.

Eq. (1) is rewritten in a more compact form as

$$m_k = Hx_k + c_k + e_k, \quad (2)$$

where the correction c_k due to the combined effect of bias and scale factor errors is defined as

$$c_k \equiv \Delta H_k x_k + b_k. \quad (3)$$

A recursive relation of the correction c_k is modeled similar to a random walk process as

$$\begin{aligned} c_{k+1} &= c_k + v_k, \\ E[v_k] &= 0, \quad E[v_k v_j^T] = Q \delta_{kj} \quad \text{and} \quad E[v_k e_j^T] = 0 \quad \forall k, j, \end{aligned} \quad (4)$$

where the stationary noise v_k represents modeling uncertainties. The objective is to obtain an unbiased predictor estimate \hat{c}_k of the correction c_k so that the signal m_k can be calibrated at each sample.

Let us construct a filter that calibrates each signal with respect to the remaining redundant signals. The filter input is the parity vector p_k of the uncalibrated signal m_k , which is defined (Potter & Suman, 1977; Ray & Desai, 1986; Ray & Luck, 1991) as

$$p_k = Vm_k, \quad (5)$$

where the rows of the projection matrix $V \in \mathcal{R}^{(\ell-n) \times \ell}$ form an orthonormal basis of the left null space of the scale factor matrix $H \in \mathcal{R}^{\ell \times n}$ in Eq. (1), i.e.,

$$VH = 0_{(\ell-n) \times n} \quad \text{and} \quad VV^T = I_{(\ell-n) \times (\ell-n)} \quad (6)$$

and the columns of V span the parity space that contains the parity vector. A combination of Eqs. (2), (5) and (6) yields

$$p_k = Vc_k + \varepsilon_k, \quad (7)$$

where the noise $\varepsilon_k \equiv Ve_k$ having $E[\varepsilon_k] = 0$ and $E[\varepsilon_k \varepsilon_j^T] \equiv VR_k V^T \delta_{kj}$.

Remark 2. If the scale factor error matrix ΔH_k belongs to the column space of H , then the parity vector p_k is independent of the true value x_k of the measured variable. Therefore, for $\|V\Delta H_k x_k\| \ll \|Vb_k\|$ that includes small scale factor errors, the calibration filter operates approximately independent of x_k .

Now we proceed to construct a recursive algorithm to predict the estimated correction \hat{c}_k based on the principle of a linear least-squares estimator that has the structure of an optimal minimum-variance filter (Jazwinski, 1970; Gelb, 1974) and uses Eqs. (4) and (7)

$$\begin{aligned} \hat{c}_{k+1} &= \hat{c}_k + K_k \gamma_k \quad \text{given } \hat{c}_0, \\ P_{k+1} &= (I - K_k V)P_k + Q \quad \text{given } P_0 \text{ and } Q, \\ K_k &= P_k V^T (V[R_k + P_k]V^T)^{-1} \quad \text{given } R_k, \end{aligned} \quad (8)$$

$$\gamma_k \equiv p_k - V\hat{c}_k \quad \text{innovation.}$$

Upon evaluation of the unbiased estimated correction \hat{c}_k , the uncalibrated signal m_k is compensated to yield the calibrated signal y_k as

$$y_k = m_k - \hat{c}_k. \quad (9)$$

Using Eqs. (5) and (9), the innovation γ_k in Eq. (8) can be expressed as the projection of the calibrated signal y_k onto the parity space, i.e.,

$$\gamma_k = Vy_k. \quad (10)$$

By setting $\Gamma_k \equiv K_k V$, we obtain an alternative form of the recursive relations in Eq. (8) as

$$\begin{aligned} \hat{c}_{k+1} &= \hat{c}_k + \Gamma_k y_k \quad \text{given } \hat{c}_0, \\ P_{k+1} &= (I - \Gamma_k)P_k + Q \quad \text{given } P_0 \text{ and } Q, \\ \Gamma_k &= P_k V^T (V[R_k + P_k]V^T)^{-1} V \quad \text{given } R_k. \end{aligned} \quad (11)$$

Remark 3. The matrix $(V[R_k + P_k]V^T)^{-1}$ in Eqs. (8) and (11) exists because the rows of V are linearly independent, $R_k > 0$, and $P_k \geq 0$.

Next, we obtain an unbiased weighted least-squares estimate \hat{x}_k of the measured variable x_k based on the calibrated signal y_k as

$$\hat{x}_k = (H^T R_k^{-1} H)^{-1} H^T R_k^{-1} y_k. \quad (12)$$

Remark 4. The inverse R_k^{-1} of the measurement covariance matrix R_k serves as the weighting matrix for generating the estimate \hat{x}_k and is used as a filter matrix.

Remark 5. Compensation of a (slowly varying) undetected error in the j th signal out of ℓ redundant signals causes the magnitude $|_j \hat{c}_k|$ in the correction vector \hat{c}_k to be the largest. Therefore, a limit check on each element of \hat{c}_k allows detection and isolation of the degraded signal(s). The bounds of limit check, which could be different for individual elements of \hat{c}_k , are selected by trade-off between the probability of false alarms and the allowable error in the estimate \hat{x}_k of the measured variable.

2.1. Degradation monitoring

Following Eq. (12), we define the residual η_k of the calibrated signal y_k as

$$\eta_k = y_k - H\hat{x}_k. \quad (13)$$

The residuals represent a measure of relative degradation of individual signals. For example, under normal conditions, all calibrated signals are clustered together, i.e., $\|\eta_k\| \approx 0$, although this may not be true for the residuals $(m_k - H\hat{x}_k)$ of uncalibrated signals.

While large abrupt changes in excess of the error threshold are easily detected and isolated by a standard diagnostics procedure (e.g., Ray & Desai, 1986), small errors (e.g., slow drift) can be identified from the a posteriori probability of failure of the calibrated signals. The a posteriori probability of failure is recursively computed from the history of residuals based on the following

ternary hypotheses:

$$\begin{aligned} H^0: & \text{Normal behavior with a priori conditional density function } {}_j f^0(\bullet) \equiv {}_j f(\bullet|H^0), \\ H^1: & \text{High (positive) failure with a priori conditional density function } {}_j f^1(\bullet) \equiv {}_j f(\bullet|H^1), \\ H^2: & \text{Low (negative) failure with a priori conditional density function } {}_j f^2(\bullet) \equiv {}_j f(\bullet|H^2), \end{aligned} \quad (14)$$

where the left subscript refers to the j th signal for $j = 1, 2, \dots, \ell$, and the right superscript indicates the normal or failure mode. The density function for each residual is determined a priori from experimental data and/or instrument manufacturers' specifications. Only one test is needed here to accommodate both positive and negative failures in contrast to the binary hypotheses that require two tests.

Let us apply the recursive relations for multi-level hypotheses testing of single variables, derived in the Appendix, to each signal residual. Then, for the j th signal at the k th sampling instant, a posteriori probability of failure ${}_j \Pi_k$ is obtained following Eq. (A.17) as

$$\begin{aligned} {}_j \Psi_k &= \left(\frac{{}_j p + {}_j \Psi_{k-1}}{2(1 - {}_j p)} \right) \left(\frac{{}_j f^1(j\eta_k) + {}_j f^2(j\eta_k)}{{}_j f^0(j\eta_k)} \right), \\ {}_j \Pi_k &= \frac{{}_j \Psi_k}{1 + {}_j \Psi_k}, \end{aligned} \quad (15)$$

where ${}_j p$ is the a priori probability of failure of the j th sensor during one sampling period, and the initial condition of each state, ${}_j \Psi_0$, $j = 1, 2, \dots, \ell$, needs to be specified.

Based on the a posteriori probability of failure, we now proceed to formulate a recursive relation for the measurement noise covariance matrix R_k that influences both calibration and estimation as seen in Eqs. (8)–(12). Its initial value R_0 , which is determined from experimental data and/or instrument manufacturers' specifications, provides the a priori information on individual signal channels and conforms to the normal operating mode when all calibrated signals are clustered together, i.e., $\|\eta_k\| \approx 0$. In the absence of any signal degradation, R_k remains close to its initial value R_0 . Significant changes in R_k may take place if one or more signals start degrading. The following model captures this phenomenon:

$$R_k = \sqrt{R_k^{rel}} R_0 \sqrt{R_k^{rel}} \quad \text{with } R_0^{rel} = I, \quad (16)$$

where R_k^{rel} is a positive-definite diagonal matrix representing only a posteriori relative information of the individual signal channels and is independent of the specific structure of the sensor system; R_k^{rel} is recursively generated as follows:

$$R_{k+1}^{rel} = \text{diag}[h({}_j \Pi_k)], \text{ i.e., } {}_j r_{k+1}^{rel} = h({}_j \Pi_k), \quad (17)$$

where ${}_j r_k^{rel}$ and ${}_j \Pi_k$ are, respectively, the relative variance and a posteriori probability of failure of the j th signal at the k th instant; and $h: [0,1) \rightarrow [1, \infty)$ is a continuous monotonically increasing function with boundary conditions $h(0) = 1$ and $h(\varphi) \rightarrow \infty$ as $\varphi \rightarrow 1$.

Remark 6. The implication of Eq. (17) is that credibility of a signal monotonically decreases with increase in its variance that tends to infinity as its a posteriori probability of failure approaches 1. The magnitude of the relative variance ${}_j r_k^{rel}$ is set to the minimum value of 1 for zero a posteriori probability of failure. In other words, the j th diagonal element ${}_j w_k^{rel} \equiv 1/{}_j r_k^{rel}$ of the weighting matrix $W_k^{rel} \equiv (R_k^{rel})^{-1}$ tends to zero as ${}_j \Pi_k$ approaches 1. Similarly, the relative weight ${}_j w_k^{rel}$ is set to the maximum value of 1 for ${}_j \Pi_k = 0$. Consequently, a gradually degrading sensor carries monotonically decreasing weight in the computation of the estimate \hat{x}_k in Eq. (12).

Next, we set the bounds on the states ${}_j \Psi_k$ of the recursive relation in Eq. (15). The lower limit of ${}_j \Pi_k$ (which is an algebraic function of ${}_j \Psi_k$) is set to the probability ${}_j p$ of intra-sample failure. On the other extreme, if ${}_j \Pi_k$ approaches 1, the weight ${}_j w_k^{rel}$ (that approaches zero) may prevent fast restoration of a degraded sensor following its recovery. Therefore, the upper limit of ${}_j \Pi_k$ is set to $(1 - {}_j \alpha)$ where ${}_j \alpha$ is the allowable probability of false alarms of the j th signal. Consequently, the function $h(\bullet)$ in Eq. (17) is restricted to the domain $[{}_j p, (1 - {}_j \alpha)]$ to account for probabilities of intra-sampling failures and false alarms. Following Eq. (15), the lower and upper limits of the states ${}_j \Psi_k$ thus become ${}_j p/(1 - {}_j p)$ and $(1 - {}_j \alpha)/{}_j \alpha$, respectively. Consequently, the initial state in Eq. (15) is set as ${}_j \Psi_0 = {}_j p/(1 - {}_j p)$ for $j = 1, 2, \dots, \ell$.

3. Sensor calibration in a commercial-scale fossil power plant

The calibration filter, derived above, has been tested in a 320 MWe coal-fired supercritical power plant for on-line sensor calibration and estimation at the throttle steam condition of $\sim 1040^\circ\text{F}$ (560°C) and ~ 3625 psia (25.0 MPa). The set of redundant signals is generated by four temperature sensors installed at different spatial locations of the main steam header that carries superheated steam from the steam generator into the high-pressure turbine via the throttle valves and governor valves (Stultz & Kitto, 1992). Since these sensors are not spatially collocated, they can be asynchronous under transient conditions due to the time-varying transport lag. The filter simultaneously calibrates the sensors to generate a time-dependent estimate of the throttle steam temperature that is spatially averaged over the main

steam header. This information on the estimated average temperature is used for health monitoring and damage prediction in the main steam header as well as for coordinated feedforward–feedback control of the power plant under both steady-state and transient operations (Kallappa, Holmes & Ray, 1997; Kallappa & Ray, 2000). The filter software is hosted in a Pentium platform and can be transported to other platforms.

The readings of all the four temperature sensors have been collected over a period of 100 h at the sampling frequency of once every one minute. The collected data, after bad data suppression (e.g., elimination of obvious outliers following built-in tests such as limit check and rate check), shows that each sensor exhibits temperature fluctuations resulting from the inherent thermal-hydraulic noise and process transients as well as the instrumentation noise. For this specific application, the parameters, functions, and matrices of the calibration filter are selected as described below.

3.1. Filter parameters and functions

We start with the filter parameters and functions that are necessary for degradation monitoring. In this application, each element of the residual vector η_k of the calibrated signal vector y_k is assumed to be Gaussian distributed that assures existence of the likelihood ratios in Eq. (15). The structures of the a priori conditional density functions are chosen as follows:

$$\begin{aligned} {}_j f^0(\varphi) &= \frac{1}{\sqrt{2\pi} {}_j \sigma} \exp\left(-\frac{1}{2} \left(\frac{\varphi}{{}_j \sigma}\right)^2\right), \\ {}_j f^1(\varphi) &= \frac{1}{\sqrt{2\pi} {}_j \sigma} \exp\left(-\frac{1}{2} \left(\frac{\varphi - {}_j \theta}{{}_j \sigma}\right)^2\right), \\ {}_j f^2(\varphi) &= \frac{1}{\sqrt{2\pi} {}_j \sigma} \exp\left(-\frac{1}{2} \left(\frac{\varphi + {}_j \theta}{{}_j \sigma}\right)^2\right), \end{aligned} \quad (18)$$

where ${}_j \sigma$ is the standard deviation, and ${}_j \theta$ and $-{}_j \theta$ are the thresholds for positive and negative failures, respectively, of the j th residual.

Since it is more convenient to work in the natural-log scale for Gaussian distribution than for the linear scale, an alternative to Eq. (17) is to construct a monotonically decreasing continuous function $g: (-\infty, 0) \rightarrow (0,1]$ in lieu of the monotonically increasing continuous function $h: [0,1) \rightarrow [1, \infty)$ so that

$W_{k+1}^{rel} \equiv (R_{k+1}^{rel})^{-1} = \text{diag}[g(\ln {}_j \Pi_k)]$, i.e., the weight

$${}_j w_{k+1}^{rel} \equiv ({}_j r_{k+1}^{rel})^{-1} = g(\ln {}_j \Pi_k). \quad (19)$$

The structure of the continuous function $g(\bullet)$ is chosen to be piecewise linear as given below:

$$g(\varphi) = \begin{cases} w^{\max} & \text{for } \varphi \leq \varphi^{\min}, \\ \frac{(\varphi^{\max} - \varphi)w^{\max} + (\varphi - \varphi^{\min})w^{\min}}{\varphi^{\max} - \varphi^{\min}} < 0, & \text{for } -\infty \leq \varphi^{\min} \leq \varphi \leq \varphi^{\max} \\ w^{\min} & \text{for } \varphi \geq \varphi^{\max}. \end{cases} \quad (20)$$

The function $g(\bullet)$ maps the space of ${}_j\Pi_k$ in the natural log scale into the space of the relative weight ${}_jw_{k+1}^{rel}$ of individual sensor data. The domain of $g(\bullet)$ is restricted to $[\ln({}_jp), \ln(1 - {}_j\alpha)]$ to account for probability ${}_jp$ of intra-sampling failure and probability ${}_j\alpha$ of false alarms for each of the four sensors. The range of $g(\bullet)$ is selected to be $[_jw^{\min}, 1]$ where a positive minimum weight (i.e., ${}_jw^{\min} > 0$) allows the filter to restore a degraded sensor following its recovery. Numerical values of the filter parameters, ${}_j\sigma$, ${}_j\theta$, ${}_jp$, ${}_j\alpha$, and ${}_jw^{\min}$ are presented below:

- Standard deviations of the a priori Gaussian density functions of the four temperature sensors are

$$\begin{aligned} {}_1\sigma &= 4.1^\circ\text{F} (2.28^\circ\text{C}); & {}_2\sigma &= 3.0^\circ\text{F} (1.67^\circ\text{C}); \\ {}_3\sigma &= 2.4^\circ\text{F} (1.33^\circ\text{C}); & {}_4\sigma &= 2.8^\circ\text{F} (1.56^\circ\text{C}). \end{aligned}$$

The initial condition for the measurement noise covariance matrix is set as: $R_0 = \text{diag}[_j\sigma]$.

The failure threshold parameters are selected as: ${}_j\theta = {}_j\sigma/2$ for $j = 1, 2, 3, 4$.

- The probability of intra-sampling failure is assumed to be identical for all four sensors as they are similar in construction and operate under identical environment. Operation experience at the power plant shows that the mean life of a resistance thermometer sensor, installed on the mean steam header, is about 700 days of continuous operation. For a sampling interval of one minute, this information leads to

$${}_jp \approx 10^{-6} \quad \text{for } j = 1, 2, 3, 4.$$

- The probability of false alarms is selected in consultation with the plant operating personnel. On the average, each sensor is allowed to generate a false alarm after approximately 700 days of continuous operation. For a sampling interval of one minute, this information leads to

$${}_j\alpha \approx 10^{-6} \quad \text{for } j = 1, 2, 3, 4.$$

- To allow restoration of a degraded sensor following its recovery, the minimum weight is set as

$${}_jw_{\min} \approx 10^{-3} \quad \text{for } j = 1, 2, 3, 4.$$

3.2. Filter matrices

After conversion of the sensor data into engineering units, the scale factor matrix in Eq. (1) becomes

$$H = [1 \ 1 \ 1 \ 1]^T.$$

Consequently, following Potter and Suman (1977) and Ray and Luck (1991), the parity space projection matrix in Eq. (6) becomes

$$V = \begin{bmatrix} \sqrt{\frac{3}{4}} & -\sqrt{\frac{1}{12}} & -\sqrt{\frac{1}{12}} & -\sqrt{\frac{1}{12}} \\ 0 & \sqrt{\frac{2}{3}} & -\sqrt{\frac{1}{6}} & -\sqrt{\frac{1}{6}} \\ 0 & 0 & \sqrt{\frac{1}{2}} & -\sqrt{\frac{1}{2}} \end{bmatrix}.$$

Remark 7. In the event of a sensor being isolated as faulty, sensor redundancy reduces to 3, for which

$$H = \begin{bmatrix} 1 \\ 1 \\ 1 \end{bmatrix} \quad \text{and} \quad V = \begin{bmatrix} \sqrt{\frac{2}{3}} & -\sqrt{\frac{1}{6}} & -\sqrt{\frac{1}{6}} \\ 0 & \sqrt{\frac{1}{2}} & -\sqrt{\frac{1}{2}} \end{bmatrix}.$$

The ratio, $R_k^{-1/2}QR_k^{-1/2}$, of covariance matrices Q and R_k in Eqs. (4) and (1), respectively, largely determines the characteristics of the minimum variance filter in Eq. (8) or Eq. (11). The filter gain Γ_k increases with a larger ratio $R_k^{-1/2}QR_k^{-1/2}$ and vice versa. Since the initial steady-state value R_0 is specified and R_k^{el} is recursively generated thereon to calculate R_k via Eq. (16), the choice is left only for selection of Q . As a priori information on Q may not be available, its choice relative to R_0 is a design feature. In this application, we have set $Q = R_0$.

3.3. Filter performance based on experimental data

The filter was tested on-line in the power plant over a continuous period of six months except for two short breaks during plant shutdown. The test results showed that the filter was able to calibrate each sensor under both pseudo-steady-state and transient conditions under closed-loop control of throttle steam temperature. The calibrated estimate of the throttle steam temperature was used for plant monitoring and control under steady state, load following, start-up, and scheduled shutdown. No natural failure of the sensors occurred during the test period and there was no evidence of any drift of the estimated temperature.

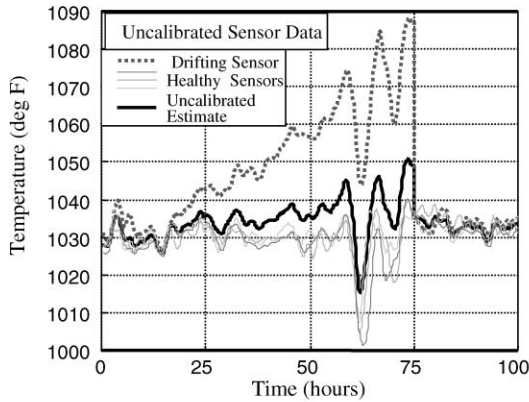
In addition to testing under on-line plant operation, simulated faults have been injected into the plant data to evaluate efficacy of the calibration filter under sensor failure conditions. Based on the data of four temperature sensors collected at 1 min over a period of 0–100 h, the following case of simulated sensor degradation is presented below:

3.3.1. Drift error and recovery in a single sensor

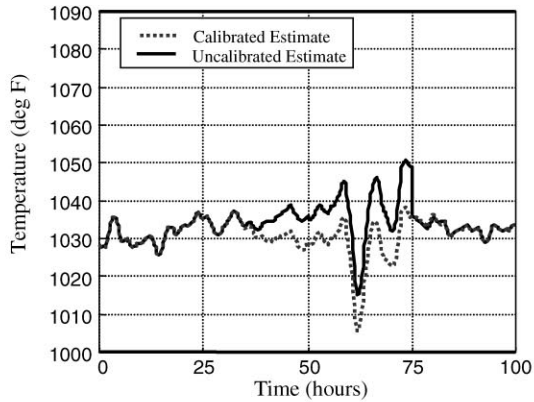
Starting at 12.5 h, a drift error was injected into the data stream of Sensor #1 in the form of an additive ramp at the rate of 1.167°F (0.648°C)/h. The injected fault was brought to zero at 75 h signifying that the faulty amplifier in the sensor hardware was corrected and reset.

Simulation results in the six plates of Fig. 1 exhibit how the calibration filter responds to a gradual drift in one of the four sensors while the remaining three are normally functioning. Plate (a) in Fig. 1 shows the re-

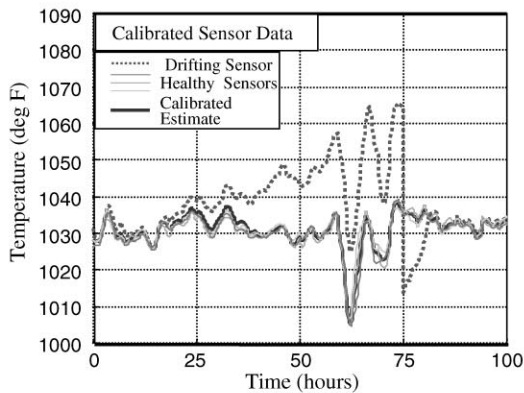
sponse of the four uncalibrated sensors as well as the estimate generated by simple averaging (i.e., fixed identical weights) of these four sensor readings at each sample. The sensor data profile includes transients lasting from ~ 63 to ~ 68 h. From time 0 to 12.5 h when no fault is injected, all sensor readings are clustered together. Therefore, the uncalibrated estimate, shown by a thick solid line, is in close agreement with all four sensors during the period 0 to 12.5 h. Sensor #1, shown by the dotted line, starts drifting at 12.5 h while the remaining three sensors,



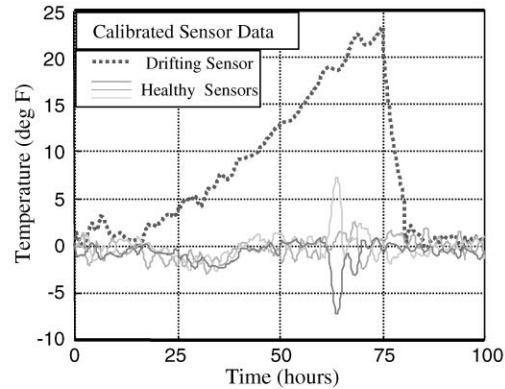
(a) Uncalibrated Sensor Data and the Estimate



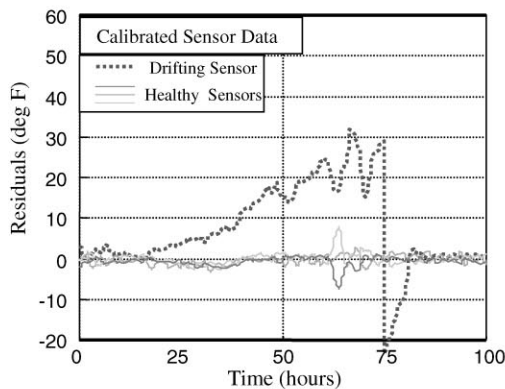
(d) Calibrated and Uncalibrated Estimates



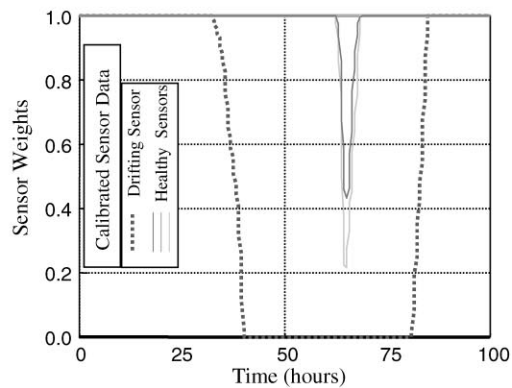
(b) Calibrated Sensor Data and the Estimate



(e) Correction for Sensor Data Calibration



(c) Residuals of the Calibrated Sensor Data



(f) Weights for Sensor Calibration

Fig. 1. Filter Performance for Drift Error in a Sensor.

shown by thin solid lines, stay healthy. Consequently, the uncalibrated estimate starts drifting at one quarter of the drift rate of Sensor #1 because of equal weighting of all sensors in the absence of the calibration filter. Upon termination of the drift fault at 75 h, when Sensor #1 is brought back to the normal state, the uncalibrated estimate resumes its normal state close to all four sensors for the remaining period from 75 to 100 h.

Plate (b) in Fig. 1 shows the response of the four calibrated sensors as well as the estimate generated by weighted averaging (i.e., varying non-identical weights) of these four sensor readings at each sample. The calibrated estimate in Plate (b) stays with the remaining three healthy sensors even though Sensor #1 is gradually drifting. Plate (f) shows that, after the fault injection, Sensor #1 is weighted less than the remaining sensors. This is due to the fact that the residual η_k^1 (see Eq. (13)) of Sensor #1 in Plate (c) increases in magnitude with the drift error. The profile of ${}_1w^{rel}$ in Plate (f) is governed by its nonlinear relationship with η_k^1 given by Eqs. (15), (19) and (20). As seen in Plate (f), ${}_1w^{rel}$ initially changes very slowly to ensure that it is not sensitive to small fluctuations in sensor data due to spurious noise such as those resulting from thermal-hydraulic turbulence. The significant reduction in ${}_1w^{rel}$ takes place after about 32 h and eventually reaches the minimum value of 10^{-3} when η_k^1 is sufficiently large. Therefore, the calibrated estimate \hat{x}_k is practically unaffected by the drifting sensor and stays close to the remaining three healthy sensors. In essence, \hat{x}_k is the average of the three healthy sensors. Upon restoration of Sensor #1 to the normal state, the calibrated signal ${}_1y_k$ temporarily goes down because of the large value of correction ${}_1\hat{c}_k$ at that instant as seen in Plate (e). However, the adaptive filter quickly brings back ${}_1\hat{c}_k$ to a small value and thereby the residual ${}_1\eta_k$ is reduced and the original weight (i.e., ~ 1) is regained. Calibrated and uncalibrated estimates are compared in Plate (d) that shows a difference of about 10°F (4.5°C) over a prolonged period.

In addition to the accuracy of the calibrated estimate, the filter provides fast and smooth recovery from abnormal conditions under both steady-state and transient operations of the power plant. For example, during the transient disturbance after about 65 h, the steam temperature undergoes a relatively large swing. Since the sensors are not spatially collocated, their readings are different during plant transients as a result of (time-varying) transport lag in the steam header. Plate (f) shows that the weights of two sensors out of the three healthy sensors are temporarily reduced while the remaining healthy sensor enjoys the full weight and the drifting Sensor #1 has practically no weight. As the transients are over, three healthy sensors resume the full weight. The cause of weight reduction is the relatively large residuals of these two sensors as seen in Plate (c). During this period, the two affected sensors undergo modest corrections: one is positive and the other negative as seen in

Plate (e) so that the calibrated values of the three healthy sensors are clustered together. The health monitoring system and the plant control system rely on calibrated estimates of signals such as spatially averaged throttle steam temperature (Kallappa et al., 1997; Kallappa & Ray, 2000; Holmes & Ray, 1998, 2000).

An important feature of the calibration filter is that it reduces the deviation of the drifting Sensor #1 from the remaining sensors as seen from a comparison of its responses in Plates (a) and (b). This is very important from the perspectives of fault detection and isolation for the following reason. In an uncalibrated system, Sensor #1 might have been isolated as faulty due to accumulation of the drift error. In contrast, the calibrated system makes Sensor #1 temporarily ineffective without eliminating it as faulty. A warning signal can be easily generated when the weight of Sensor #1 diminishes to a small value. This action will draw the attention of maintenance personnel for possible repair or adjustment. Since the estimate \hat{x}_k is not contaminated by the degraded sensor, a larger detection delay can be tolerated. Consequently, the allowable threshold for fault detection can be safely increased to reduce the probability of false alarms.

4. Summary and conclusions

This paper develops and validates an adaptive filter for on-line calibration of redundant signals and estimation of the measured plant variable. The redundancy may consist of both sensor signals and/or analytical measurements that are derived from other sensor signals and physical characteristics or a model of the plant. All redundant signals are simultaneously calibrated by additive corrections that are recursively estimated. A weighted least-squares estimate of the measured variable is generated in real time where the weighting matrix is adaptively adjusted as a function of the a posteriori probability of failure of the calibrated signals. The effects of intra-sample failure and probability of false alarms are taken into account in the recursive filter that has been tested for on-line calibration of four redundant sensors of the throttle steam temperature in a commercial-scale fossil power plant. In addition, simulated scenarios of sensor failure have been investigated by injecting faults into a set of data collected from an operating fossil power plant. The filter exhibits speed and accuracy during both steady state and transient operations of the power plant. It also shows fast recovery when the fault is corrected or naturally mitigated. The software is presently hosted in a Pentium platform and is portable to other commercial platforms. The important features of this real-time adaptive filter are summarized below:

- A model of the physical process is not necessary for calibration and estimation if sufficient redundancy

of sensor data and/or analytical measurements is available.

- All signals are simultaneously calibrated on-line to compensate for their relative errors.
- The weights of individual signals for computation of a least-square estimate are adaptively updated as functions of the respective a posteriori probabilities of failure.

The proposed calibration and estimation filter can enhance the Instrumentation & Control System Software in tactical and transport aircraft, and nuclear and fossil power plants. However, a limitation of this filter is its inability to handle common mode faults (i.e., similar faults, possibly due to a common source, in all or a majority) of redundant sensors because the filter algorithm relies on the relative error among the individual signals. Additional information (e.g., analytic redundancy) is needed to deal with common-mode faults.

Acknowledgements

The research work reported in this paper has been supported in part by: Office of Naval Research under Grant No. N00014-97-1-0786; and National Academy of Sciences under a Research Fellowship award to the first author.

Appendix: Multiple hypotheses testing based on independent observations of a single variable

Let $\{\eta_k, k = 1, 2, 3, \dots\}$ be independent observations of a single variable (e.g., residual of a signal) at consecutive sampling instants. We assume M distinct possible modes of failure in addition to the normal mode of operation that is designated as the mode 0. Thus, at each sampling instant, there are $(M + 1)$ mutually exclusive and exhaustive modes. Each of these $(M + 1)$ modes is treated as a Markov state. The hypotheses of failure of $(M + 1)$ modes at the k th sample are defined as follows:

H_k^0 : Normal behavior with a priori density function

$$f^0(\bullet) \equiv f(\bullet|H^0),$$

H_k^i : Abnormal behavior with a priori density function

$$f^i(\bullet) \equiv f(\bullet|H^i), \quad i = 1, 2, \dots, M. \tag{A.1}$$

We assume a one–one correspondence between the set of $(M + 1)$ modes and the set of their failure hypotheses $H_k^j, j = 0, 1, 2, \dots, M$. In the sequel, the terms, mode and hypothesis, are synonymously used.

We define the a posteriori probability π_k^j of the j th mode at the k th sample as

$$\pi_k^j \equiv P[H_k^j | Z_k], \quad j = 0, 1, 2, \dots, M, \tag{A.2}$$

based on the cumulative information $Z_k \equiv \bigcap_{i=1}^k z_i$ over k samples where the events $z_i \equiv \{\eta_i \in B_i\}$ are mutually independent and B_i is the region of interest at the i th sample. The problem is to derive a recursive relation for a posteriori probability Π_k of any one of the M failure modes at the k th sample

$$\Pi_k \equiv P\left[\bigcup_{j=1}^M H_k^j | Z_k\right] = \sum_{j=1}^M P[H_k^j | Z_k] \Rightarrow \Pi_k = \sum_{j=1}^M \pi_k^j. \tag{A.3}$$

Eq. (A.3) holds because of the exhaustive and mutually exclusive properties of the Markov states, $H_k^j, j = 1, 2, \dots, M$. To construct a recursive relation for Π_k , we introduce the following definitions:

Joint probability:

$$\xi_k^j \equiv P[H_k^j, Z_k], \tag{A.4}$$

a priori probability:

$$\lambda_k^j \equiv P[z_k | H_k^j], \tag{A.5}$$

transition probability:

$$a_k^{i,j} \equiv P[H_k^j | H_{k-1}^i]. \tag{A.6}$$

Then, because of independence of the events z_k and Z_{k-1} , Eq. (A.4) takes the following form:

$$\begin{aligned} \xi_k^j &= P[H_k^j, z_k, Z_{k-1}] \\ &= P[z_k | H_k^j] P[H_k^j, Z_{k-1}]. \end{aligned} \tag{A.7}$$

Furthermore, the exhaustive and mutually exclusive properties of the Markov states $H_k^j, j = 0, 1, 2, \dots, M$, and independence of Z_{k-1} and H_k^j lead to

$$\begin{aligned} P[H_k^j, Z_{k-1}] &= \sum_{i=0}^M P[H_k^j, H_{k-1}^i, Z_{k-1}] \\ &= \sum_{i=0}^M P[Z_{k-1} | H_{k-1}^i] P[H_k^j | H_{k-1}^i] P[H_{k-1}^i] \\ &= \sum_{i=0}^M P[H_k^j | H_{k-1}^i] P[H_{k-1}^i, Z_{k-1}]. \end{aligned} \tag{A.8}$$

The following recursive relation is obtained from a combination of Eqs. (A.4)–(A.8) as

$$\xi_k^j = \lambda_k^j \sum_{i=0}^M a_k^{i,j} \xi_{k-1}^i. \tag{A.9}$$

We introduce a new term

$$\psi_k^j \equiv \frac{\xi_k^j}{\xi_k^0} \tag{A.10}$$

that reduces to the following form by use of Eq. (A.9)

$$\psi_k^j = \left(\frac{\lambda_k^j}{\lambda_k^0} \right) \left(\frac{a_k^{0,j} + \sum_{i=1}^M a_k^{i,j} \psi_{k-1}^i}{a_k^{0,0} + \sum_{i=1}^M a_k^{i,0} \psi_{k-1}^i} \right), \quad (\text{A.11})$$

to obtain the a posteriori probability π_k^j in Eq. (A.2) in terms of ζ_k^j and ψ_k^j as

$$\begin{aligned} \pi_k^j &= \frac{P[H_k^j, Z_k]}{P[Z_k]} = \frac{P[H_k^j, Z_k]}{\sum_{i=0}^M P[H_k^i, Z_k]}, \\ &= \frac{\zeta_k^j}{\zeta_k^0 + \sum_{i=1}^M \zeta_k^i} = \frac{\psi_k^j}{1 + \sum_{i=1}^M \psi_k^i}. \end{aligned} \quad (\text{A.12})$$

A combination of Eqs. (A.3) and (A.12), leads to the a posteriori probability Π_k of failure as

$$\Pi_k = \frac{\Psi_k}{1 + \Psi_k} \quad \text{with } \Psi_k \equiv \sum_{j=1}^M \psi_k^j. \quad (\text{A.13})$$

The above expressions can be realized by a simple recurrence relation under the following four assumptions:

- **Assumption A.1:** At the starting point (i.e., $k = 0$), all signals operate in the normal mode, i.e., $P[H_0^0] = 1$ and $P[H_0^j] = 0$ for $j = 1, 2, \dots, M$. Therefore, $\zeta_0^0 = 1$ and $\zeta_0^j = 0$ for $j = 1, 2, \dots, M$.
- **Assumption A.2:** Transition from the normal mode to any abnormal mode is equally likely. That is, if p is the a priori probability of failure during one sampling interval, then $a_k^{0,0} = 1 - p$ and $a_k^{0,i} = p/M$ for $i = 1, 2, \dots, M$, and all k .
- **Assumption A.3:** No transition takes place from an abnormal mode to the normal mode implying that $a_k^{i,0} = 0$ for $i = 1, 2, \dots, M$, and all k . The implication is that a failed sensor does not return to the normal mode (unless replaced or repaired).
- **Assumption A.4:** Transition from an abnormal mode to any abnormal mode including itself is equally likely. That is, $a_k^{i,j} = 1/M$ for $i, j = 1, 2, \dots, M$, and all k .

A recursive relation for Ψ_k is generated based on the above assumptions and using the expression in Eq. (A.11) as

$$\begin{aligned} \psi_k^j &= \frac{p + \sum_{i=1}^M \psi_{k-1}^i}{(1-p)M} \left(\frac{\lambda_k^j}{\lambda_k^0} \right) \quad \text{given } \psi_0^j = 0 \\ &\text{for } j = 1, 2, \dots, M, \end{aligned} \quad (\text{A.14})$$

which is simplified by the use of the relation $\Psi_k \equiv \sum_{i=1}^M \psi_k^i$ in Eq. (A.13) as

$$\Psi_k = \left(\frac{p + \Psi_{k-1}}{(1-p)M} \right) \sum_{j=1}^M \frac{\lambda_k^j}{\lambda_k^0} \quad \text{given } \Psi_0 = 0. \quad (\text{A.15})$$

If the probability measure associated with each abnormal mode is absolutely continuous relative to that associated with the normal mode, then the ratio λ_k^j/λ_k^0 of a priori probabilities converges to a Radon–Nikodym derivative as the region B_k in the expression $z_k \equiv \{\eta_k \in B_k\}$ ap-

proaches zero measure (Wong & Hajek, 1985). This Radon–Nikodym derivative is simply the likelihood ratio $f^j(\eta_k)/f^0(\eta_k)$, $j = 1, 2, \dots, M$, where $f^j(\bullet)$ is the a priori density function conditioned on the hypothesis H^j , $j = 0, 1, 2, \dots, M$. Accordingly, Eq. (A.15) becomes

$$\Psi_k = \left(\frac{p + \Psi_{k-1}}{(1-p)M} \right) \sum_{j=1}^M \frac{f^j(\eta_k)}{f^0(\eta_k)} \quad \text{given } \Psi_0 = 0. \quad (\text{A.16})$$

For the specific case of two abnormal hypotheses (i.e., $M = 2$) representing positive and negative failures, the recursive relations for Ψ_k and Π_k in Eqs. (A.16) and (A.13) become

$$\begin{aligned} \Psi_k &= \left(\frac{p + \Psi_{k-1}}{2(1-p)} \right) \left(\frac{f^1(\eta_k) + f^2(\eta_k)}{f^0(\eta_k)} \right) \\ \Pi_k &= \frac{\Psi_k}{1 + \Psi_k} \end{aligned} \quad \left. \vphantom{\begin{aligned} \Psi_k &= \left(\frac{p + \Psi_{k-1}}{2(1-p)} \right) \left(\frac{f^1(\eta_k) + f^2(\eta_k)}{f^0(\eta_k)} \right)} \right\} \quad \text{given } \Psi_0 = 0. \quad (\text{A.17})$$

References

- Daly, K. C., Gai, E., & Harrison, J. V. (1979). Generalized likelihood test for FDI in redundant sensor configurations. *Journal of Guidance and Control*, 2(1), 9–17.
- Deckert, J.C., Fisher, J.L., Laning, D.B., & Ray, A. (1983). Signal validation for nuclear power plants. *ASME Journal of Dynamic Systems, Measurement and Control* 105(1) 240–29.
- Desai, M., Deckert, J. C., & Deyst, J. J. (1979). Dual sensor identification using analytic redundancy. *Journal of Guidance and Control*, 2(3), 213–220.
- Gelb, A. Ed. (1974). *Applied optimal estimation*. Cambridge, MA: MIT Press.
- Holmes, M., & Ray, A. (1998). Fuzzy damage mitigating control of mechanical structures. *ASME Journal of Dynamic Systems, Measurement and Control*, 120(2), 249–256.
- Holmes, M., & Ray, A. (2000). Fuzzy damage mitigating control of power plants, *IEEE Transactions on Control Systems Technology*, in press.
- Jazwinski, A. H. (1970). *Stochastic processes and filtering theory*. New York: Academic Press.
- Kallappa, P., Holmes, M., & Ray, A. (1997). Life extending control of fossil power plants for structural durability and high performance. *Automatica*, 33(6), 1101–1118.
- Kallappa, P., & Ray, A. (2000). Fuzzy wide-range control of fossil power plants for life extension and robust performance. *Automatica*, 36(1), 69–82.
- Potter, J. E., & Suman, M. C. (1977). Thresholdless redundancy management with arrays of skewed instruments. Integrity in Electronic Flight Control Systems, *NATO AGARDOGRAPH-224* (pp. 15-1–15-15).
- Ray, A., Geiger, R., Desai, M., & Deyst, J. (1983). Analytic redundancy for on-line fault diagnosis in a nuclear reactor. *AIAA Journal of Energy*, 7(4), 367–373.
- Ray, A., & Desai, M. (1986). A redundancy management procedure for fault detection and isolation. *ASME Journal of Dynamic Systems, Measurement and Control*, 108(3), 248–254.
- Ray, A., & Luck, R. (1991). Signal validation in multiply-redundant systems. *IEEE Control Systems Magazine*, 11(2), 44–49.
- Stultz, S.C., & Kitto, J.B. (Eds.), (1992). *STEAM: Its generation and use* (40th ed.). Baberton, OH: Babcock & Wilcox.
- Wong, E., & Hajek, B. (1985). *Stochastic processes in engineering systems*. New York: Springer.

Asok Ray earned the Ph.D. degree in Mechanical Engineering from Northeastern University, Boston, MA in 1976, and also graduate degrees in each discipline of Electrical Engineering, Mathematics, and Computer Science. Dr. Ray joined the Pennsylvania State University in July 1985, and is currently a Professor of Mechanical Engineering. Prior to joining Penn State, Dr. Ray held research and academic positions at Massachusetts Institute of Technology and Carnegie-Mellon University as well as research and management positions at GTE Strategic Systems Division, Charles Stark Draper Laboratory, and MITRE Corporation. Dr. Ray has been also a Senior Research Fellow at NASA Lewis Research Center under a National Academy of Sciences award. Dr. Ray's research experience and interests include: Fault-accommodating and robust control systems, Modeling and analysis of thermo-mechanical fatigue and creep in both deterministic and stochastic settings, Intelligent instrumentation for real-time distributed processes, and Control and optimization of continuously varying and discrete-event dynamic systems, as applied to Aeronautics and Astronautics, Undersea Vehicles and Surface Ships, Power and Processing plants, and Autonomous Manufacturing. Dr. Ray has authored or co-authored three hundred research publications including over one hundred and thirty five scholarly articles in refereed journals and research monographs. Dr. Ray is a Fellow of ASME, an Associate Fellow of AIAA, and a Senior Member of IEEE.

For a recent photograph of Asok Ray please refer to *Automatica* 36(1), pp. 36.

Shashi Phoha earned the Ph.D. degree in Mathematical Statistics from Michigan State University, East Lansing, MI in 1976 and the M.S. degree in Operations Research from Cornell University, Ithaca, NY in 1973. Dr. Phoha is the Head of the Information Science Division and Assistant Director of the Applied Research Laboratory and a Professor of Electrical and Computer Engineering at Penn State University. Her research focuses on information sciences, which bring together ideas from logic, operations research, formal languages, automata theory, dynamic systems, and control theory in diverse applications. She has diverse experience in multi-organizational collaborative research and in scientific analysis of distributed information. Drawing on her broad scientific background and multidisciplinary research collaborations, she has made outstanding contributions to the scientific analysis of distributed information for decision support, multi-stage coordination and intelligent control of interacting processes in complex dynamic systems. Some of her recent innovations are implemented in the National Information Infrastructure Test bed which is a university/industry partnership, funded by DARPA, for developing web based mechanisms for sensor and model based health monitoring and failure prognosis in operating machinery. She has established other innovative research directions for understanding ocean and environmental physics through analysis of correlated time-series data collected by a self reconfiguring network of undersea robotic vehicles.

For a recent photograph of Shashi Phoha please refer to *Automatica* 36(1), pp. 36.